Theoretical Foundations of Chemical Engineering, Vol. 34, No. 1, 2000, pp. 13–21.
Translated from Teoreticheskie Osnovy Khimicheskoi Tekhnologii, Vol. 34, No. 1, 2000, pp. 16–24.

Heat Exchange during a Slow Flow of a Liquid between Coaxial Conical Surfaces

L. M. Ul'ev

Kharkov State Polytechnical University, ul. Frunze 21, Kharkov, 310002 Ukraine

Received February 11, 1998

Abstract—The problem of convective heat transfer during a slow liquid flow in conical annular channels is considered. For third-kind thermal boundary conditions, the problem is solved by separation of variables. The temperature distribution is represented as the product of an infinite Whittaker-function series in lateral coordinate and an exponential of longitudinal coordinate. Heat transfer in a variable-width annular conical channel is analyzed by stepwise approximation. Optimization of the distributing sections of extruder dies is shown to be possible.

Extrusion processing of polymers is sometimes controlled by heat exchange [1]. Therefore, to optimize the extruder design and process parameters, it is necessary to study convective heat transfer in extruder die channels. In most extruder dies, there are channels formed by coaxial conical surfaces [2, 3]. For a polymer flowing in such channels, joint solution to the hydrodynamic and heat-transfer equations is very difficult and can be carried out only by numerical methods. The problem of convective heat transfer for a non-Newtonian liquid flowing in an annular conical channel was formulated in [4]. A numerical method to solve this problem was suggested in [5], but the solution itself was not reported.

Under processing conditions, some molten polymers behave as Newtonian liquids [6]. For typical flow rates and rheological and physical properties of such liquids ($Q \approx 5.0 \times 10^{-5}$ m^3/s, $\mu \approx 10^3$ Pa s, $\rho \approx 2500$ kg/m^3, $\lambda \approx 0.2$ W/(m K), $\Delta T_{rheol} \approx 6$ K, and $c \approx 2000$ J/(kg K)) and for typical channel geometry ($L \leq 0.5$ m, $h \approx 10^{-2}$–10^{-1} m; see Fig. 1), the Name–Griffith and Reynolds numbers are far less than unity ($Gn \ll 1$, $Re \ll 1$) [7]. Therefore, the flow can be considered to be laminar, and dissipative effects can be neglected. Since the Peclet number $Pe \geq 100$, we can also neglect a variation of the conductive heat flux along the flow direction relative to the convective heat flux [8].

The above assumptions allow us to simplify the system of convective-heat-transfer equations and to obtain analytical solutions for some important cases. An analysis of such solutions would eliminate the need for expensive full-scale experimentation and no less expensive numerical simulation.

Let us consider convective heat transfer in an annular conical channel of a constant width [7]. Flows in such a channel are convenient to examine in the biconical coordinates with the origin at the vertex of the outer cone (Fig. 1), which are defined as [9]

$$z' = R\cos\alpha + X\sin\alpha, \quad (1)$$

$$y' = (R\sin\alpha - X\cos\alpha)\sin\varphi, \quad (2)$$

$$x' = (R\sin\alpha - X\cos\alpha)\cos\varphi. \quad (3)$$

The above assumptions lead to a system of hydrodynamic equations [7], which, in terms of the dimensionless variables

$$\xi = R/h, \quad \xi_0 = R_0/h, \quad \chi = X/h, \quad V_0 = Q/S_0,$$
$$v = V_R/V_0, \quad \Pi = (P - P_0)h/(\mu V_0),$$

and

$$\sigma = \xi\sin\alpha - \chi\cos\alpha,$$

where

$$S_0 = \pi(2R_0\sin\alpha - h\cos\alpha)h$$

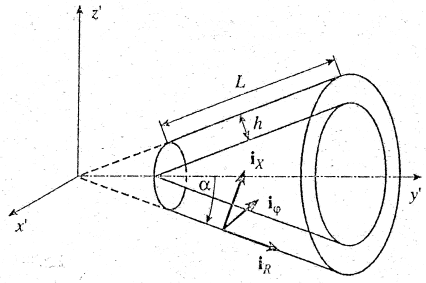

Fig. 1. Geometry of a conical channel of a constant width. $\mathbf{i}_R$, $\mathbf{i}_X$, and $\mathbf{i}_\varphi$ are the unit vectors of the biconical coordinates.

0040-5795/00/3401-0013$25.00

is the inlet cross-sectional area of the channel, is written as

$$\frac{\partial \Pi}{\partial \xi} = \frac{1}{\sigma}\frac{\partial}{\partial \chi}\left(\sigma \frac{\partial v}{\partial \chi}\right), \quad (4)$$

$$\frac{\partial \Pi}{\partial \chi} = \frac{\cos(\alpha)\sin(\alpha)}{\sigma^2} v, \quad (5)$$

$$\frac{\partial}{\partial \xi}(\sigma v) = 0 \quad (6)$$

with sticking boundary conditions and $\Pi = 0$ at the channel inlet.

With the Lame coefficients calculated in [7], the heat-transfer equation for the flow between conical surfaces is

$$\mathrm{Pe} v \frac{\partial \Theta}{\partial \xi} = \frac{1}{\sigma}\frac{\partial}{\partial \chi}\left(\sigma \frac{\partial \Theta}{\partial \chi}\right), \quad (7)$$

where

$$\mathrm{Pe} = \frac{V_0 h}{a}, \quad \Theta = \frac{T - T_0}{T_0}.$$

Evaluation of the Brun number gives

$$\mathrm{Br} = \frac{\lambda}{\lambda_w}\frac{h_w}{(R - R_0)}\mathrm{Pr}^{0.33}\mathrm{Re}^{0.5} \le 0.01$$

for most of the channel. Therefore, the third-kind boundary conditions [10]

$$\frac{\partial \Theta}{\partial \chi} = \mathrm{Bi}_1(\Theta - \Theta_1) \text{ at } \chi = 0 \quad (8)$$

and

$$\frac{\partial \Theta}{\partial \chi} = -\mathrm{Bi}_2(\Theta - \Theta_2) \text{ at } \chi = 1, \quad (9)$$

as well as the channel-inlet condition

$$\Theta = 0 \text{ at } \xi = \xi_0, \quad (10)$$

are applicable as a satisfactory approximation. Here, $\mathrm{Bi} = Kh/\lambda$ is the Biot number, and K is the local heat-transfer coefficient [8].

To reduce the heat-transfer equation to the dimensionless form, we used $\Delta T = T_0 - 0 = T_0$ to rule out any limitations on the ambient temperatures at unrelated boundaries.

In cases important in practice ($\xi \tan\alpha \gg \chi$), the system of equations (4)–(6) has the following solution [7]:

$$v = \frac{6(2\xi_0 \sin\alpha - \cos\alpha)}{\cos\alpha - 2\xi \sin\alpha}(\chi^2 - \chi), \quad (11)$$

$$\Pi = -\frac{6(\cos\alpha - 2\xi_0 \sin\alpha)}{\sin\alpha} \ln\frac{1 - 2\xi\tan\alpha}{1 - 2\xi_0 \tan\alpha}. \quad (12)$$

In view of equation (11), equation (7) takes the form

$$\frac{6\mathrm{Pe}(2\xi_0 \sin\alpha - \cos\alpha)}{\cos\alpha - 2\xi\sin\alpha}(\chi^2 - \chi)\frac{\partial \Theta}{\partial \xi} = \frac{\partial^2 \Theta}{\partial \chi^2}. \quad (13)$$

Equation (13) with boundary conditions (8) and (9) describes the temperature distribution in the channel.

To solve equation (13) with boundary conditions (8)–(10) by separation of variables, we replace the dependent variable Θ by Φ, which is defined as

$$\Theta(\xi, \chi) = \Phi(\xi, \chi) + \frac{\mathrm{Bi}_1\mathrm{Bi}_2(\Theta_2 - \Theta_1)}{\mathrm{Bi}_1(\mathrm{Bi}_2 + 1) + \mathrm{Bi}_2}\chi + \frac{\mathrm{Bi}_1(\mathrm{Bi}_2 + 1)\Theta_1 + \mathrm{Bi}_2\Theta_2}{\mathrm{Bi}_1(\mathrm{Bi}_2 + 1) + \mathrm{Bi}_2}. \quad (14)$$

With function Φ, the form of equation (13) is unchanged, and inhomogeneous boundary conditions (8) and (9) are transformed to homogeneous ones:

$$\frac{\partial \Phi}{\partial \chi} = \mathrm{Bi}_1 \Phi \text{ at } \chi = 0, \quad (15)$$

$$\frac{\partial \Phi}{\partial \chi} = -\mathrm{Bi}_2 \Phi \text{ at } \chi = 1. \quad (16)$$

Channel-inlet condition (10) ($\xi = \xi_0$, $0 \le \chi \le 1$) appears as

$$\Phi_0(\chi) = -\frac{\mathrm{Bi}_1\mathrm{Bi}_2(\Theta_2 - \Theta_1)}{\mathrm{Bi}_1(\mathrm{Bi}_2 + 1) + \mathrm{Bi}_2}\chi - \frac{\mathrm{Bi}_1(\mathrm{Bi}_2 + 1)\Theta_1 + \mathrm{Bi}_2\Theta_2}{\mathrm{Bi}_1(\mathrm{Bi}_2 + 1) + \mathrm{Bi}_2} = \Phi(\xi_0, \chi). \quad (17)$$

Next, we represent the function Φ as a product $\Phi(\xi, \chi) = Y(\xi)\Psi(\chi)$ and obtain from equation (13)

$$6\mathrm{Pe}\frac{2\xi_0 \sin\alpha - \cos\alpha}{\cos\alpha - 2\xi\sin\alpha}\frac{dY}{Y} = \gamma^2 d\xi, \quad (18)$$

$$\Psi'' - \gamma^2(\chi^2 - \chi)\Psi = 0, \quad (19)$$

where γ^2 is the separation constant, which is always positive, because, under the conditions of the problem, the polymer temperature in the channel is finite at any ξ.

The solution of equation (18) is

$$Y = A\exp\left[-\frac{\gamma^2(\cos\alpha - 2\xi\sin\alpha)^2}{24\mathrm{Pe}\sin\alpha(2\xi_0\sin\alpha - \cos\alpha)}\right], \quad (20)$$

where A is an arbitrary constant.

By substituting $t = 2\chi - 1$ and $\gamma = 4\mu$ into equation (19) and the corresponding boundary conditions, we obtain

$$\Psi'' + \mu^2(1 - t^2)\Psi = 0, \quad (21)$$

$$\frac{\partial \Psi}{\partial t} = \frac{1}{2}\mathrm{Bi}_1 \Psi \text{ at } t = -1, \quad (22)$$

$$\frac{\partial\Psi}{\partial t} = -\frac{1}{2}\mathrm{Bi}_2\Psi \quad \text{at } t = 1. \tag{23}$$

Substituting $y = \mu t^2$ and $\Psi = \varphi\mu^{-1/4}t^{-1/2}$ into equation (21) gives

$$\varphi'' + \left(-\frac{1}{4} + \frac{\mu}{4y} + \frac{3}{16y^2}\right)\varphi = 0. \tag{24}$$

Equation (24) is a particular case of the Whittaker equation [11]

$$\varphi'' + \left(-\frac{1}{4} + \frac{k}{y} + \frac{\frac{1}{4} - m^2}{y^2}\right)\varphi = 0 \tag{25}$$

with $k = \mu/4$ and $m = 1/4$.

The solution of equation (25) is given by the linearly independent Whittaker functions $M_{k,m}(y)$ and $M_{k,-m}(y)$ [11]. The general solution of equation (24) is then

$$\varphi = C_1 e^{-y/2} y^{3/4} {}_1F_1\left(\frac{3-\mu}{4}, \frac{3}{2}; y\right) + C_2 e^{-y/2} y^{1/4} {}_1F_1\left(\frac{1-\mu}{4}, \frac{1}{2}; y\right), \tag{26}$$

where ${}_1F_1(\alpha, \varepsilon; x)$ is a degenerate hypergeometric function and C_1 and C_2 are arbitrary constants. Equation (21) then takes the form

$$\Psi(t) = C_1\sqrt{\mu}e^{-\mu t^2/2} {}_1F_1\left(\frac{3-\mu}{4}, \frac{3}{2}; \mu t^2\right) + C_2 e^{-\mu t^2/2} {}_1F_1\left(\frac{1-\mu}{4}, \frac{1}{2}; \mu t^2\right). \tag{27}$$

Substituting solution (26) into boundary conditions (22) and (23) gives the expression for determining the eigenvalues of boundary problem (21)–(23):

$$\sqrt{\mu}(D_1 D_2 + D_3 D_4) = 0, \tag{28}$$

where

$$D_1 = \left(\frac{\mathrm{Bi}_2}{2} + 1 - \mu\right) {}_1F_1\left(\frac{3-\mu}{4}, \frac{3}{2}; \mu\right) + \frac{1}{3}\mu(3-\mu) {}_1F_1\left(\frac{7-\mu}{4}, \frac{5}{2}; \mu\right),$$

$$D_2 = \left(\frac{\mathrm{Bi}_1}{2} - \mu\right) {}_1F_1\left(\frac{1-\mu}{4}, \frac{1}{2}; \mu\right) + \mu(1-\mu) {}_1F_1\left(\frac{5-\mu}{4}, \frac{3}{2}; \mu\right),$$

$$D_3 = \left(\frac{\mathrm{Bi}_1}{2} + 1 - \mu\right) {}_1F_1\left(\frac{3-\mu}{4}, \frac{3}{2}; \mu\right) + \frac{1}{3}\mu(3-\mu) {}_1F_1\left(\frac{7-\mu}{4}, \frac{5}{2}; \mu\right),$$

$$D_4 = \left(\frac{\mathrm{Bi}_2}{2} - \mu\right) {}_1F_1\left(\frac{1-\mu}{4}, \frac{1}{2}; \mu\right) + \mu(1-\mu) {}_1F_1\left(\frac{5-\mu}{4}, \frac{3}{2}; \mu\right).$$

Having found the eigenvalues μ_n as the roots of equation (28), we obtain the system of the eigenfunctions of the problem:

$$\Psi_n = \sqrt{\mu_n}te^{-\mu_n t^2/2} {}_1F_1\left(\frac{3-\mu_n}{4}, \frac{3}{2}; \mu_n t^2\right) + B_n e^{-\mu_n t^2/2} {}_1F_1\left(\frac{1-\mu_n}{4}, \frac{1}{2}; \mu_n t^2\right), \tag{29}$$

where

$$B_n = \frac{\sqrt{\mu_n}D_3(\mu_n)}{D_2(\mu_n)}, \quad n = 0, 1, 2, \ldots, \infty.$$

From equation (21) with boundary conditions (22) and (23), one can deduce that the eigenfunctions Ψ_n are orthogonal and $(1-t^2)$-weighted in the interval $[-1, 1]$.

The solution of problem stated by (13), (15), and (16) is found as the sum of all particular solutions. In view of $t = 2\chi - 1$, it is written as

$$\Phi(\xi, t) = \sum_{n=0}^{\infty} A_n \exp\left[-\frac{2\mu_n^2(\cos\alpha - 2\xi\sin\alpha)^2}{3\mathrm{Pe}\sin\alpha(2\xi_0\sin\alpha - \cos\alpha)}\right]\Psi_n. \tag{30}$$

The coefficients A_n can be derived from the orthogonality property of the eigenfunctions and condition (17). For $\xi = \xi_0$, we obtain

$$\Phi_0(t) = \sum_{n=0}^{\infty} A_n \exp\left[-\frac{2\mu_n^2(\cos\alpha - 2\xi_0\sin\alpha)^2}{3\mathrm{Pe}\sin\alpha(2\xi_0\sin\alpha - \cos\alpha)}\right]\Psi_n. \tag{31}$$

Multiplication of both sides of expression (31) by $(1 - t^2)\Psi_n$, followed by integration between -1 and 1, gives

$$A_n = \exp\left[\frac{2\mu_n^2(\cos\alpha - 2\xi_0\sin\alpha)^2}{3\mathrm{Pe}\sin\alpha(2\xi_0\sin\alpha - \cos\alpha)}\right] \times \frac{\int_{-1}^{1}\Phi_0(t)(1-t^2)\Psi_n(t)dt}{\|\Psi_n\|^2} \tag{32}$$

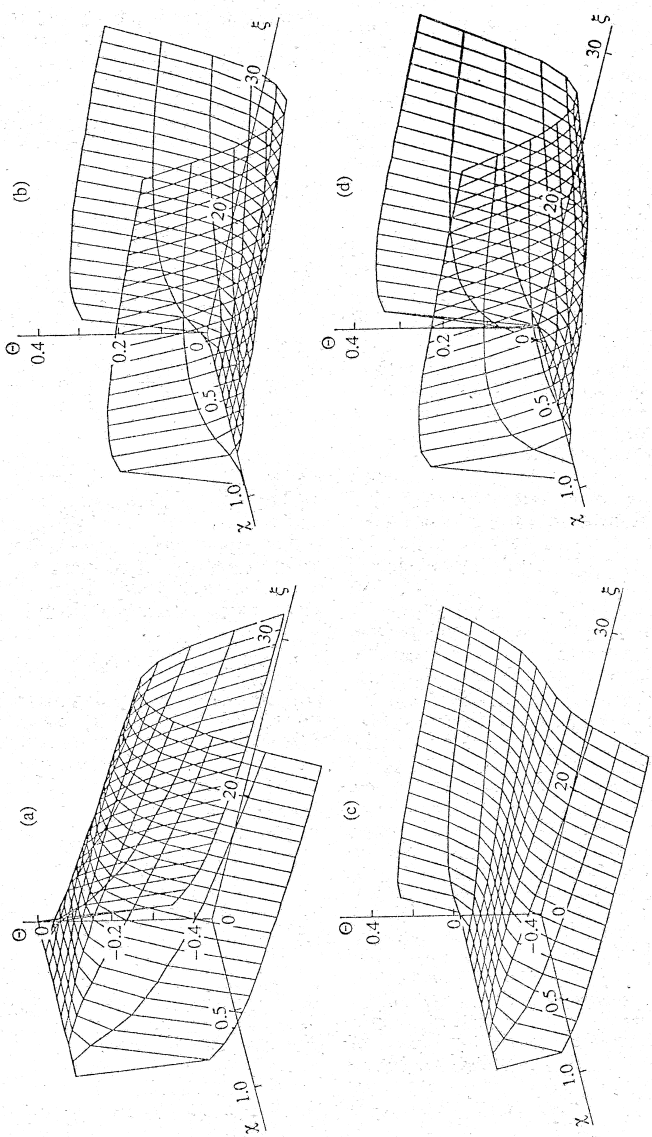

Fig. 2. Distribution of Θ in the channel at Pe = 1300, $Bi_1 = Bi_2 = 20$, $\Theta(\xi_0, \chi) = 0$, $\xi_0 = 12.9$, and $\xi_1 = 32.9$. (a) $\Theta_1 = \Theta_2 = -0.5$ (for the ambient temperature), $\alpha = 15°$; (b) $\Theta_1 = \Theta_2 = 0.5$, $\alpha = 15°$; (c) $\Theta_1 = 0.5$, $\Theta_2 = -0.5$, $\alpha = 15°$; and (d) $\Theta_1 = \Theta_2 = 0.5$, $\alpha = 40°$, Pe = 470.

$$= \exp\left[\frac{2\mu_n^2(\cos\alpha - 2\xi_0\sin\alpha)^2}{3\mathrm{Pe}\sin\alpha(2\xi_0\sin\alpha - \cos\alpha)}\right]A_n',$$

where $\|\Psi_n\|^2 = \int_{-1}^{1}(1-t^2)\Psi_n^2\,dt$ is the squared norm of the eigenfunctions.

In terms of variables ξ and χ, the solution of problem ((13), (8), and (9)) is

$$\Theta(\xi,\chi) = \Phi(\xi_0,\chi)$$

$$+\left\{\sum_{n=0}^{\infty}A_n'\exp\left\{\frac{8\mu_n^2(\xi-\xi_0)[\cos\alpha-(\xi+\xi_0)\sin\alpha]}{3\mathrm{Pe}(2\xi_0\sin\alpha-\cos\alpha)}\right.\right.$$

$$\left.-\frac{\mu_n(2\chi-1)^2}{2}\right\} \qquad (33)$$

$$\times\left\{\sqrt{\mu_n}(2\chi-1)_1F_1\left[\frac{3-\mu_n}{4},\frac{3}{2};\mu_n(2\chi-1)^2\right]\right.$$

$$\left.\left.+B_{n1}F_1\left[\frac{1-\mu_n}{4},\frac{1}{2};\mu_n(2\chi-1)^2\right]\right\}\right\}.$$

This solution enables us to study heat transfer in the channel as a function of process parameters. Let us consider symmetrical melt cooling at $\mathrm{Pe} \approx 1300$, $\mathrm{Bi}_1 = \mathrm{Bi}_2 = 20$, $\Theta(\xi_0,\chi) = 0$, $\Theta_1 = \Theta_2 = -0.5$, $\xi_0 = 12.9$, $\xi_1 = 32.9$, and $\alpha = 15°$. Near the channel inlet, the liquid rapidly cools at the flow periphery. In the central zone of the flow, temperature is virtually invariable because of low heat conductivity (Fig. 2). As the liquid flows further, its mean velocity

$$\bar{v} = (2\xi_0\sin\alpha - \cos\alpha)/(2\xi\sin\alpha - \cos\alpha)$$

decreases, causing the cooling of a greater volume of the liquid far from the walls. The heat fluxes at the boundaries, $q_1 = -\mathrm{Bi}_1(\Theta - \Theta_1)$ and $q_2 = \mathrm{Bi}_2(\Theta - \Theta_2)$, rapidly fall in modulus, because the liquid temperature decreases at the walls but remains symmetrical (Fig. 2).

A similar situation is obtained during symmetrical heating. In both cases, the weight-average liquid temperature

$$\bar{\Theta} = \frac{12}{\cos\alpha - 2\xi\sin\alpha}\int_0^1(\chi^2-\chi)\Theta(\chi,\xi) \qquad (34)$$

$$\times(\xi\sin\alpha - \chi\cos\alpha)d\chi$$

varies almost linearly by about 10%. When heat transfer is asymmetrical (Fig. 2c), the heat fluxes at the walls are nearly equal (Fig. 3), and the mean temperature is constant.

As the angular opening of the cone is increased at fixed ξ and flow rate, the mean flow velocity decreases because of growing the cross-sectional area of the channel. The Peclet number Pe (i.e., heat-transfer rate) also decreases. A decrease in flow velocity causes an increase in the dwell time of the liquid in the channel, and an increase in α to 40° (Fig. 2d) leads to a larger heat-exchange surface and, therefore, to better heating of the liquid. In this case, the mean liquid temperature is higher by ~20%, although heat fluxes in most of the channel are lower than those at $\alpha = 15°$.

The solution suggested here allows the design of the conical distributing section of an underwater granulator to be optimized so that it can provide, for example, minimum temperature variation in the channel.

We now consider two cases of heat transfer.

Case 1. There is no thermal insulation between the channel and water flowing around the granulator legs, and natural heat transfer occurs at the outer boundary. For the outer boundary, $\mathrm{Bi}_1 = 20$; for the inner boundary, $\mathrm{Bi}_2 = 40$. The inlet melt temperature T_0 is 463 K, air temperature $T_1 = 293$ K, and water temperature T_2 is 280 K. $Q \approx 5.6 \times 10^{-5}$ m^3/s, $\alpha = 15°$, $h = 0.03$ m, $\xi_0 = 12.9$, and $\xi_1 = 32.9$.

Case 2. The channel is thermally insulated from water carrying away the granules ($\mathrm{Bi}_2 = 0.25$). At the outer surface, high-rate convective heat transfer between water and the heat carrier takes place with $T_1 = 463$ K and $\mathrm{Bi}_1 = 40$. The inlet melt temperature T_0 is 463 K.

In the first case (Fig. 4a), the temperature distribution is similar to that considered above (Fig. 2a). The only difference is that water cooling at the outer surface is more intense; that is, the heat flux q_2 is higher throughout the channel length (Fig. 5a).

In the second case, the heat flux through the outer surface is negligible (Fig. 5b); the colder layer, resulting from heat exchange with water, has time to extend only over a third of the channel width (Fig. 4b).

In the first and second cases, the mean temperature is, respectively, 10 and 0.3% lower than the initial temperature (Fig. 6).

The solution suggested can be applied to study mass transfer in liquids flowing in annular channels between conical surfaces with nonparallel generators. Such channels have found wider application than constant-width channels. A pressure drop in a channel between concentric conical surfaces with vertices on one side of the channel can be calculated by a stepwise approximation of the channel with constant-width annular conical fragments [7]. This method, no more sophisticated than others, does not approximate a convergent or divergent flow by a straight-line stream.

Let us use such an approach to study heat transfer in a channel formed by circular conical surfaces with $2\alpha_1 = 42°$, $2\alpha_2 = 30°$, $h_0 = 0.03$ m, $R_0 = 0.279$ m, and $L = 0.6$ m. Parameter r (Fig. 7), liquid flow rate, and

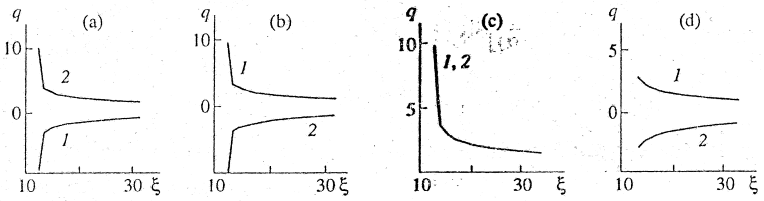

Fig. 3. Distribution of (*1*) q_1 and (2) q_2 along the channel. The conditions (a–d) are the same as in Fig. 2.

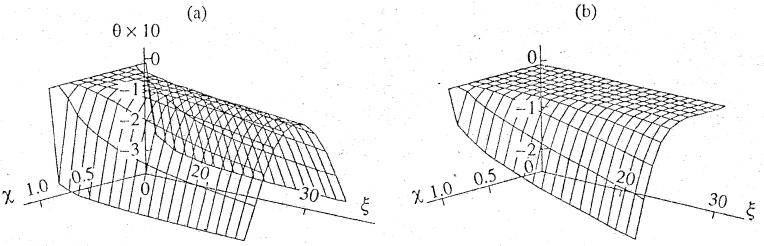

Fig. 4. Distribution of Θ in the distributing channel of the underwater granulator in the (a) first and (b) second cases.

temperatures are considered to be constant ($T_0 = 463$ K, $T_1 = 293$ K, and $T_2 = 280$ K). Heat-transfer coefficients K_1 and K_2 are 133.3 and 266.6 W/(m² K) (for $h = h_0$, $\mathrm{Bi}_1 = 20$, and $\mathrm{Bi}_2 = 40$).

Assume that the inner conical surface consists of N conical fragments whose generators are parallel to the generator of the outer surface and are equal to L/N. We then have a channel composed of N constant-width coaxial conical channels. In our cases, the major contribution to heat exchange is from convective heat transfer (Stanton number $\mathrm{St} = K/(\rho c V_0) \le 10^{-2}$). Therefore, the width of each of the channels has to be selected such that the length-average liquid flow velocities in the approximating and original fragments are equal. This is attained when the approximating and original fragments have equal length-average cross-sectional areas. The mean cross-sectional area of a constant-width conical channel with length $\Delta L = L/N$ is

$$S_0 = \frac{\pi}{\Delta L}\int_{R_0}^{R_0+\Delta L} h(2R\sin\alpha - h\cos\alpha)dR = \pi[h(2R_0 + L/N)\sin\alpha - h^2\cos\alpha]. \quad (35)$$

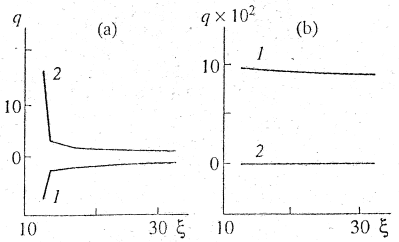

Fig. 5. Distribution of (*1*) q_1 and (2) q_2 along the channel for the (a) first and (b) second cases.

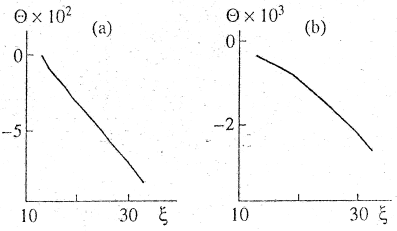

Fig. 6. Distribution of Θ along the channel for the (a) first and (b) second cases.

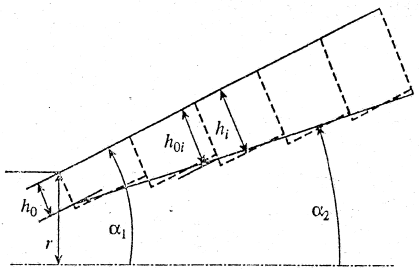

Fig. 7. Approximation of a variable-width annular channel by constant-width annular fragments.

The mean cross-sectional area of a channel formed by conical surfaces with angular openings $2\alpha_1$ and $2\alpha_2$ is given by

$$S_1 = \frac{\pi}{\Delta L}\int_{R_0}^{R_0+\Delta L}[2Rh(R)\sin\alpha - h^2(R)\cos\alpha]dR$$

$$= \pi\{(2R_0 + L/N)(h_0 - R_0\tan\beta)(\sin\alpha_1 - \cos\alpha_1\tan\beta) + \left[R_0^2 + \frac{L}{N}R_0 + \frac{1}{3}\left(\frac{L}{N}\right)^2\right] \quad (36)$$

$$\times(2\sin\alpha_1 - \cos\alpha_1\tan\beta)\tan\beta - (h_0 - R_0\tan\beta)^2\cos\alpha_1\},$$

where $h(R) = h_0 + (R - R_0)\tan\beta$, $\beta = \alpha_1 - \alpha_2$, and h_0 is the width of the channel inlet (Fig. 7).

The width of the ith approximating fragment is derived from relationships (35) and (36):

$$h_i = \frac{(2R_i + L/N)\tan\alpha_1}{2} - \left\{\frac{(2R_i + L/N)^2\tan^2\alpha_1}{4}\right.$$

$$-(2R_i + L/N)(h_{0i} - R_i\tan\beta)(\tan\alpha_1 - \tan\beta)$$

$$-\left[R_i^2 + R_i\frac{L}{N} + \frac{1}{3}\left(\frac{L}{N}\right)^2\right] \quad (37)$$

$$\left.\times(2\tan\alpha_1 - \tan\beta)\tan\beta + (h_{0i} - R_i\tan\beta)^2\right\}^{1/2},$$

where

$$R_i = R_0 + (L/N)(i-1),$$

$$h_{0i} = h_0 + (L/N)(i-1)\tan\beta.$$

Clearly, such an approximation will not affect the length-average liquid flow velocity and the channel volume for either a channel fragment or the channel as a whole. However, the approximating and original channels will have different heat-transfer surface areas. In the case that heat transfer is dominated by the heat fluxes at the surfaces, approximation must not change the heat-transfer surface area. The h_i value is then determined from

$$h_i = h_{0i} + (L/N)(\sin\alpha_1 - \sin\alpha_2). \quad (38)$$

It was ascertained that, at $N \longrightarrow \infty$ in relationships (37) and (38), $h_i \longrightarrow h_{0i}$.

Solution (33) is applicable if each ith fragment has been reduced to the dimensionless form with its peculiar h_i value. In calculating the temperature distribution in the first fragment, we assume that the initial temperature is distributed uniformly and equal to zero. That is, condition (10) is met. The inlet liquid temperature in

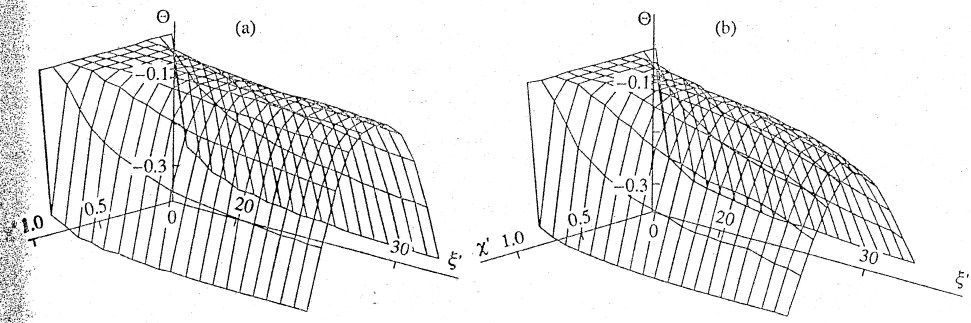

Fig. 8. Distribution of Θ in a variable-width channel: (a) $\alpha_1 = 21°$, $\alpha_2 = 15°$ and (b) $\alpha_1 = 21°$, $\alpha_2 = 32°$.

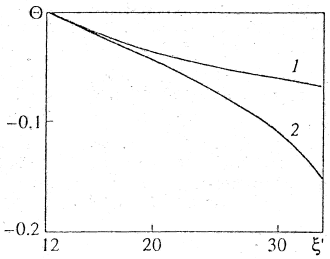

Fig. 9. Distribution of Θ along a variable-width channel: (*1*) $\alpha_1 = 21°$, $\alpha_2 = 15°$ and (*2*) $\alpha_1 = 21°$, $\alpha_2 = 32°$.

each subsequent fragment will be given by the function fitting the outlet distribution of temperature in the preceding fragment.

In this case, the liquid flow velocity decreases along the channel more sharply than it does at $\alpha_1 = \alpha_2 = 15°$ because of increasing cross-sectional area. This behavior is similar to that observed for a constant-width channel as the angular opening of the cones is raised. The ratio of the inlet and outlet cross-sectional areas is ≈2.8 for channels with $\alpha_1 = \alpha_2 = 15°$ and ≈9.8 for those with $\alpha_1 = 21°$ and $\alpha_2 = 15°$. As a consequence, the heat-transfer rate is lower in the latter case. Furthermore, the channel width is increased, and the heat-transfer surface area is decreased. Therefore, although the dwell time of the liquid in the channel increases, the central zone of the flow cools down at a lower rate (Fig. 8) than in the case depicted in Fig. 4a. There is an isomorphic correspondence between the regions of definition of Θ in Figs. 8 and 4a, which is given by the coordinate transformation

$$\xi' = \xi, \quad \chi' = \chi/[1 + (\xi - \xi_0)\tan\beta].$$

As a consequence, the mean temperature is changed less (Fig. 9).

If K significantly varies along the flow direction, it is appropriate to take K to be constant throughout an approximating fragment and equal to its mean value for this fragment.

Let us consider a channel formed by conical surfaces with $2\alpha_1 = 42°$ and $2\alpha_2 = 46°$. The heat-transfer coefficients at the surface vary as

$$K_1 = 4/[h_0 - (R - R_0)\tan\beta], \quad K_2 = 2K_1.$$

In such a channel, the mean liquid flow velocity varies only slightly along the channel, because the inlet and outlet cross-sectional areas of the channel are nearly equal. Therefore, the liquid flow velocity is higher in this case than in the cases considered above. Furthermore, the channel is narrower, and the heat-transfer surface and heat-transfer coefficients are greater. As a result, the liquid has a lower temperature throughout the channel cross section (Fig. 8) and a lower mean temperature (Fig. 9).

The solution obtained was used to optimize heat transfer in the distributing section of the extruder die of the underwater granulator used in the production of thermoplastic polymers.

NOTATION

a—thermal diffusivity, m^2/s;

c—specific heat, J/(kg K);

h—channel width, m;

$h_w = 0.05$—thickness of the channel wall, m;

K—heat-transfer coefficient, $W/(m^2 K)$;

L—length of the generator of the conical surface of a channel, m;

P, P_0—current and inlet pressures, respectively, Pa;

Q—flow rate, m^3/s;

q—heat flux, W/m^2;

R, R_0—current and inlet radial biconical coordinates, respectively, m;

S—cross-sectional area of a channel, m^2;

T, T_0—current and inlet temperatures, respectively, K;

ΔT_{rheol}—temperature change causing a substantial change in viscosity, K;

V—velocity, m/s;

X—lateral biconical coordinate, m;

x', y', z'—Cartesian coordinates, m;

α—half the angular opening of a cone, rad;

γ—constant;

λ—heat conductivity, W/(m K);

λ_w—heat conductivity of the wall, W/(m K);

μ—viscosity, Pa s;

ρ—density, kg/m^3;

$Bi = Kh/\lambda$—Biot number;

$Gn = \mu V_0^2/(\lambda\Delta T_{rheol})$—Name–Griffith number;

$Pe = V_0 h c\rho/\lambda$—Peclet number;

$Pr = \mu c/\lambda$—Prandtl number;

$Re = hV_0\rho/\mu$—Reynolds number.

REFERENCES

1. Plugar', I.Yu., Radchenko, L.B., and Senatos, V.A., Calculation of Heat Treatment Processes in Polymer Processing by Extrusion, *Teplomassoobmen. MMF-96*, Minsk, 1996, vol. 6, p. 47.

2. Tadmor, Z. and Godos, C.G., *Principles of Polymer Processing*, New York: Wiley, 1979. Translated under the title *Teoreticheskie osnovy pererabotki polimerov*, Moscow: Khimiya, 1984.

3. Torner, R.V. and Akutin, M.S., *Oborudovanie zavodov po pererabotke plastmass* (Plant Equipment for Plastic Processing), Moscow: Khimiya, 1986.

4. Trufanova, N.M., Syrchikov, I.A., and Shcherbinin, A.G., A Mathematical Heat-and-Mass Transfer Model for Polymers in a Cable Head Channel, *Teplomassoobmen. MMF-96*, Minsk, 1996, vol. 6, p. 53.

5. Rumpel', Kh., Plikhta, K., Meikel', S., and Krol', K.-I., On the Flow of Non-Newtonian Fluids, *Usp. Mekh.*, 1988, vol. 2, no. 3, p. 3.

6. Ponomarenko, V.G., Potebnya, G.F., Ul'ev, L.M., *et al.*, Determination of Rheologic Properties of High-Viscosity Liquids by Means of an Automated Capillary Viscosimeter, *Inzh.-Fiz. Zh.*, 1990, vol. 59, no. 1, p. 158.

7. Ul'ev, L.M., Slow Flows in Coaxial Conic Conduits, *Vestn. Khar'kov. Politekh. Univ., Ch. 2: Mekh. Mashinostroenie*, 1997, no. 7, p. 22.

8. Petukhov, B.S., *Teploobmen i soprotivlenie pri laminarnom techenii zhidkosti v trubakh* (Heat Exchange and Resistance at Laminar Liquid Flows in Tubes), Moscow: Energiya, 1967.

9. Gol'din, A.M. and Karamzin, V.A., *Gidrodinamicheskie osnovy protsessov tonkosloinogo separirovaniya* (Hydrodynamic Fundamentals of Thin-Film Separation), Moscow: Agropromizdat, 1985.

10. Belyaev, N.N., *Osnovy teploperedachi* (Principles of Heat Transfer), Kiev: Vishcha Shkola, 1989.

11. Kuznetsov, D.S., *Spetsial'nye funktsii* (Special Functions), Moscow: Vysshaya Shkola, 1965.